ORIGINAL ARTICLE

An experimental *Staphylococcus aureus* meningitis model for investigating induced leptomeningeal and subpial inflammation in rats: A transmission electron microscopy study

Aslan Guzel [1], Uygur Er [2], Mehmet Tatli [1], Ufuk Aluclu [3], Tuncer Ozekinci [4], Yusuf Nergiz [5], Bulent Ahishali [6], Gokhan Aktas [7], Vatan Kavak [8], Sebnem Nergiz [4], Umit Ozkan [1] & Omer Satici [9]

Neurosurgery [1], Neurology [3], Microbiology [4], Histology [5], Anatomy [8] and Biostatistics [9] Departments of Dicle University, Diyarbakir; Neurosurgery Clinic [7], Sirnak State Hospital, Sirnak; Histology-Embriology Department [6], Istanbul University, Istanbul and Second Neurosurgery Clinic [2], Diskapi Yildirim Bayezit Training and Research Hospital, Ankara, Turkey

Correspondence to: Uygur Er, MD.,
Sogutozu C., 4th Sk., No:22/7 06510, Ankara, Turkey
PHONE: +90 312 284 11 51
FAX: +90 312 316 29 29
EMAIL: uygurer@gmail.com

Submitted: July 2, 2007 *Accepted: July 14, 2007*

Key words: **electron microscopy; inflammatory reactions; meningitis model;** *Staphylococcus aureus*

Neuroendocrinol Lett 2007; **28**(5):652–658 **PMID:** 17984956 NEL280507A12

Abstract

OBJECTIVE: To evaluate leptomeningeal and subpial inflammatory responses of experimental *Staphylococcus aureus* bacteriemia following intraperitoneal and intravenous applications and to compare the inflammatory reactions in different regions of central nervous system.

MATERIAL AND METHODS: Forty anesthetized rats were divided into four groups equal in number. The rats in group-I were given 1 ml suspension of *Staphylococcus aureus* intraperitoneally. Group-II was the control group of group I; it was administrated 1 ml 0.9% NaCl in water intraperitoneally. The rats in group-III were given the same amount of bacteria intravenously. Group IV was the control group of the group-III; it was administrated 1 ml 0.9% NaCl solution intravenously. The rats were sacrificed on the 21st day. Inflammatory changes of different regions of the central nervous system were examined under transmission electron microscopy. Statistical analysis was done by using variance analysis, Bonferroni, Tamhane post hoc, Student's t and univariate tests.

RESULTS: Thoracic and occipital regions were the most vulnerable zones. Increasing of collagen tissue was the most detected inflammatory change.

CONCLUSION: This experimental model can be used for inducing subpial and leptomeningeal inflammations and it may be developed for investigations of pathogenesis of leptomeningitis during systemic infections.

Abbreviations

ANOVA	- Analysis of variance
BBB	- Blood-brain barrier
CFU	- Colony forming unit
CNS	- Central Nervous System
CSF	- Cerebrospinal fluid
DUSAM	- Dicle University Health Sciences Research Center Ethic Committee
PBS	- Phosphate-buffered saline
PMNL	- Polymorpho-nuclear leucocyte
S. aureus	- *Staphylococcus aureus*
TEM	- Transmission electron microscope
ip	- Intraperitoneally
iv	- Intravenous

INTRODUCTION

Bacterial meningitis remains as a common disease with a high mortality and morbidity despite modern antimicrobial therapy [16,18,20,23]. Meningitis associated central nervous system (CNS) lesions and neuronal death is not mediated simply by the presence of viable bacteria but occurs as a consequence of the host reaction to bacterial components [20]. Associations between inflammatory reaction of leptomeninges and subpial tissue in discrete regions of brain and spinal cord after bacteriemia are not known very well. *Staphylococcus aureus* (*S. aureus*) is one of the relatively uncommon but serious causes of bacterial meningitis accounting only 1–9% of cases of bacterial meningitis [1,14]. Mortality resulted by *S. aureus* meningitis is significantly correlated with presence of bacteriemia [17]. The aim of this study is to investigate and determine whether there is a difference in the leptomeninges and subpial tissues of different regions of the CNS in respect to the inflammatory response to an experimental bacteriemia.

MATERIALS AND METHODS

All procedures were performed in accordance with the institutional guidelines of Dicle University, Saglik Bilimleri Arastirma Merkezi, Diyarbakir, Turkey (DUSAM, Dicle University Health Sciences Research Center Ethic Committee). Forty Sprague-Dawley rats weighing 300–350 g were anesthetized with ketamine 80 mg/kg and xylasine 12.5 mg/kg. The rats divided into 4 equal groups, 10 rats in each randomly. *S. aureus* strain ATCC 25923 was used. All bacteria were passed through the mouse prior to use in the meningitis model in order to standardize their virulence measurement [4]. Bacteria were grown in brain-heart infusion broth to late log phase (Optical density at 500 nm, 0.6 to 0.8). A total of 10^8 colony forming unit (CFU) of *S. aureus* in 1ml of phosphate-buffered saline (PBS) (pH 7.4) was administrated intraperitoneally (ip) to the group I (n=10), intravenously (iv) to the group III (n=10) via the vein of the tail. The rats in group II (n=10) were given 1 ml of isotonic solution of 0.09% of NaCl in water ip; the rats in group IV (n=10) were administered 1ml of the same isotonic solution of NaCl iv via the vein of the tail.

The rats were examined daily for generally evidence of neurological dysfunction. All animals survived in all groups and were not any focal neurological deficit roughly. The rats were sacrificed on the 21st days. Brains and spinal cords were removed with overlying meninges. Leptomeninges of the frontal, temporal, occipital, cerebellar cortical, cervical, thoracic and lumbar regions were examined by transmission electron microscope (TEM) (JEOL-1010, Tokyo, Japan)

The specimens were fixed in a 2.5% of glutaraldehyde and buffered phosphate solution for 4 hours to achieve pH 7.2–7.3. Then, the specimens were fixed in a 1% of osmium tetroxide solution for an hour. After those fixation processes, they were dehydrated with increasing concentrations of acetone in water and saturated in resin epoxy (Epon 812). The resin was polymerized at 70 °C for 72 h. Control group slides were dyed in blue to identify the sites where ultrathin cuts would be made, and they were examined under the light microscope. Ultrathin slides, 70 nm in thickness, were cut by an ultramicrotome (Ultracut E; Reichert, Wien, Austria) and treated with acetate and 2% of uranilo solution, as well as Reynold's lead citrate solution. Afterwards, the specimens were examined under the TEM.

Histopathological evaluations were assessed according to some parameters including vascular changes (edema, perivascular congestion, and present of polymorphonuclear leucocytes (PMNL)), increasing of collagen fibers, thickening of basal lamina, separating junction complexes of the cells (opening of gap junctions, tight junctions, desmosomes and hemidesmosomes), edema in leptomeninges and subpial spaces [9,12,16,18,19,24,26]. The results of these findings are seen in the tables (Tables 1–6).

Results were expressed as mean of the number of inflammatory changes; and comparison among groups was made using one-way analysis of Variance (ANOVA) following Bonferroni and Tamhane post hoc tests and Student's t test. Univariate statistical test for multiple comparisons was made. In all comparisons, $p<0.05$ was considered statistically significant.

Evaluation steps

1. Brain, cerebellum and medulla spinalis were divided into eight different regions as frontal, temporal, parietal, occipital cerebral regions, cerebellar cortex, and cervical, thoracic and lumbar spinal regions for each group. Each region was evaluated in ten sections. The numbers given in the tables are the means of the number of inflammatory changes in these ten sections.
2. Inflammatory reaction was examined individually in arachnoid mater, pia mater and subpial tissue.
3. Edema, perivascular congestion, increasing of collagen fibers, thickening of basal lamina, separation of desmosomes, hemidesmosomes, gap-junction and tight-junctions, vasculitis and morphological changes of pial cells were the parameters that were used for the examination of the arachnoid and pia maters.

Table 1. Histopathological findings of arachnoid mater according to the regions of group-I.

Histopathological findings (n=10)	F	T	P	O	CE	CV	T	L
Edema	4	4	5	6	5	4	6	4
Congestion	5	4	4	6	4	5	6	5
Increasing in collagen	5	4	4	5	5	4	7	3
Thickening of basal lamina	4	3	5	6	3	3	5	3
Opening desmosomes	4	3	3	6	3	4	5	3
Opening hemidesmosomes	4	4	3	6	4	3	5	4
Opening gap-junctions	5	5	4	5	3	2	5	2
Opening tight-junctions	3	2	2	5	2	3	5	3
Vasculitis	4	3	4	6	4	4	6	3

F: Frontal, T :Temporal, P: Parietal, O: Occipital, CE: Cerebellar, CV: Cervical, T:Tohoracic, L: Lumbar

Table 2. Histopathological findings of pia mater according to the regions of group-I.

Histopathological findings (n=10)	F	T	P	O	CE	CV	T	L
Edema	3	4	5	6	4	5	4	4
Congestion	5	5	4	6	5	5	4	4
Increasing in collagen	4	5	4	5	4	4	5	3
Thickening of basal lamina	4	4	4	6	5	2	4	3
Opening desmosomes	5	4	3	5	2	2	3	2
Opening hemidesmosomes	4	5	4	5	3	3	3	4
Opening gap-junctions	4	4	4	6	4	3	2	4
Opening tight-junctions	3	4	3	6	5	3	3	2
Vasculitis	4	5	4	5	4	4	5	3
Morphological changes of pial cells	4	5	4	6	5	2	3	3

F: Frontal, T :Temporal, P: Parietal, O: Occipital, CE: Cerebellar, CV: Cervical, T:Tohoracic, L: Lumbar

4. In addition the above mentioned parameters; degeneration of myelin sheath was used for the evaluation of subpial tissue.
5. The results of arachnoid mater, pia mater and subpial tissue, and the results of different regions were compared in each group. In this step, iv and ip groups were analyzed together to reveal the regions that invaded mostly by Univariate test.
6. To determine the significance between the iv and ip groups and between the arachnoid mater, pia mater and subpial tissues, one-way variance analysis was made. Homogeneity control of variance in the groups was made by Levene statistics. Bonferroni test for variance-homogeneous groups, and Tamhane multiple comparison tests for variance-inhomogeneous groups were used to make a statistical analysis.
7. Student's t-test was used for pair-wise comparison of the mean of the results of arachnoid mater, pia mater and subpial tissue of each group.

RESULTS

There was no inflammatory reaction of any tissue of any region in the control groups II and IV. The results of inflammatory reaction of leptomeninges and subpial tissue of groups I and III (Figures 1 and 2) (Bacteria administrated ip and iv in groups I and III respectively) and according to their regions as median range of positive histopathological findings can be seen in the tables (Tables 1–6).

All the inflammatory parameters of arachnoid samples of the group-I were seen mostly in occipital and thoracic regions (Table 1). Pia mater samples of the group-I were also revealed that occipital region is the most invaded site (Table 2). Occipital region was the most invaded site in the subpial samples of the group-I; but thoracic region was also exhibited the same level of invasion according to some inflammatory parameters (Table 3).

Occipital and thoracic regions were the most invaded sites in all tissue samples in the group-III according to all parameters (Tables 4,5,6).

It can be said that, occipital and thoracic regions are the most affected; and lumbar region is the least involved sites in all groups under the light of the results of this study. It is seen that there is no statistically significant difference between the ip and iv groups. It can also be noticed that increasing in collagen tissue is the most frequently seen and loosening of the desmosomal junctions is the least frequently observed histopathological change in all groups.

DISCUSSION

A sheath of leptomeninges accompanies arteries into the brain and is related to the pathways for the drainage of interstitial fluid that plays a role in inflammatory responses in the brain [25].

Arachnoid mater is composed of an outermost layer (arachnoid barrier cell layer), presenting tightly packed

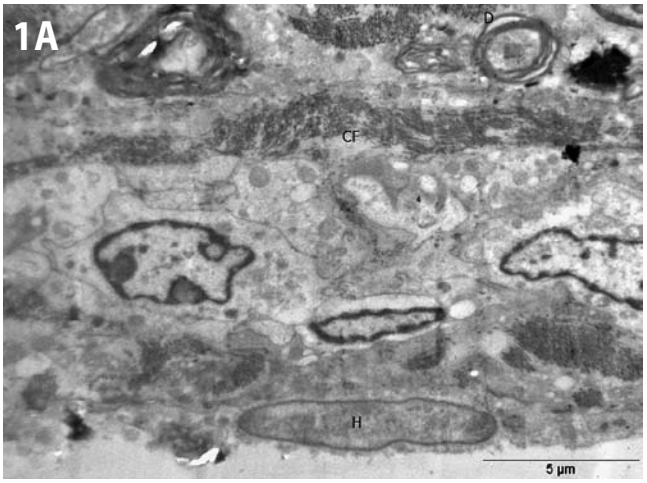

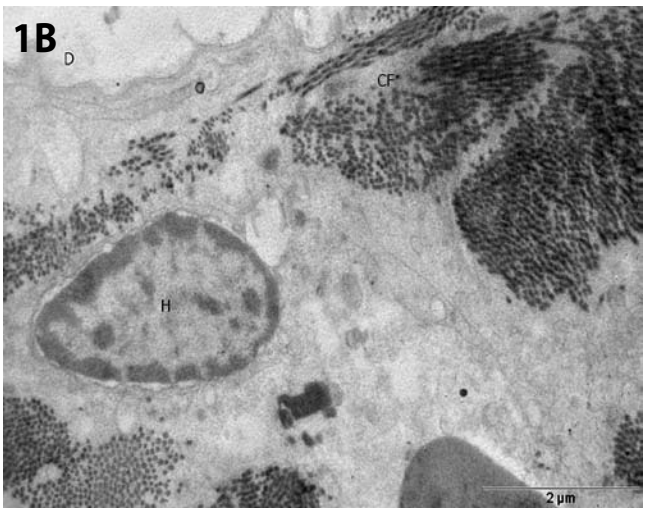

Figure 1A. Electronmicrograph of a rat of group-I in occipital region. Hematogenous cells among pial cells (H), increasing in collagen fibers (CF), and myelin degeneration (D) are seen. Bar, 5 µm. Uranyl acetate and lead citrate ×6 000.

Figure 1B. Electronmicrograph of a rat of group-I at thoracic level. Collagen accumulation (CF), tissue loss (D), and hemetagenous (H) cells are observed in subpial tissue. Bar, 2 µm. Uranyl acetate and lead citrate ×15 000.

cells, numerous tight junctions and no extra cellular collagen. This layer is considered to represent an effective morphological and physiological barrier between the cerebrospinal fluid (CSF) in the subarachnoid space and the blood circulation in the dura in view of its numerous tight junctions. The arachnoid barrier layer is always characterized by a distinct continuous basal lamina on its inner surface towards the innermost collagenous portion of the arachnoid (arachnoid reticular cell layer) [24]. The common ultrastructural features of arachnoid cells are intermediate filaments and interdigitating cytoplasmic processes which are connected by desmosomes and junction apparatus [6].

Pia mater is reflected from the surface of the brain and spinal cord onto arteries and veins, thus separating the subarachnoid space from the brain and cord [10,25].

Table 3. Histopathological findings of subpial tissue according to the regions of group-I.

Histopathological findings (n=10)	F	T	P	O	CE	CV	T	L
Edema	4	4	4	6	4	3	6	2
Congestion	5	4	5	6	5	3	5	2
Increasing in collagen	6	7	6	9	6	5	8	4
Thickening of basal lamina	6	6	6	8	6	5	6	4
Opening desmosomes	5	6	5	8	5	4	6	3
Opening hemidesmosomes	5	6	6	8	5	6	6	6
Opening gap-junctions	5	5	4	9	5	4	6	5
Opening tight-junctions	6	4	5	8	4	3	6	4
Vasculitis	3	3	4	4	3	2	5	2
Myelin degeneration	7	5	4	8	5	4	8	4

F: Frontal, T :Temporal, P: Parietal, O: Occipital, CE: Cerebellar, CV: Cervical, T:Tohoracic, L: Lumbar

Table 4. Histopathological findings of arachnoid mater according to the regions of group-III.

Histopathological findings (n=10)	F	T	P	O	CE	CV	T	L
Edema	7	6	6	9	5	7	9	6
Congestion	6	6	6	9	6	7	9	7
Increasing in collagen	7	6	5	9	6	7	9	5
Thickening of basal lamina	6	6	6	9	6	6	9	5
Opening desmosomes	6	6	5	9	5	5	6	5
Opening hemidesmosomes	6	6	6	9	8	5	8	5
Opening gap-junctions	7	5	6	9	6	4	9	6
Opening tight-junctions	5	5	4	8	4	5	9	5
Vasculitis	7	6	6	9	6	7	9	5

F: Frontal, T :Temporal, P: Parietal, O: Occipital, CE: Cerebellar, CV: Cervical, T:Tohoracic, L: Lumbar

Table 5. Histopathological findings of pia mater according to the regions of group-III.

Histopathological findings (n=10)	F	T	P	O	CE	CV	T	L
Edema	6	6	5	7	5	5	8	3
Congestion	7	6	5	7	6	5	8	5
Increasing in collagen	6	4	6	7	5	6	8	4
Thickening of basal lamina	8	5	7	8	6	6	8	5
Opening desmosomes	7	3	4	6	3	4	6	4
Opening hemidesmosomes	4	5	5	6	3	3	6	3
Opening gap-junctions	6	4	5	7	6	4	6	3
Opening tight-junctions	6	4	4	7	4	6	8	3
Vasculitis	7	6	6	6	5	5	7	4
Morphological changes of pial cells	7	6	6	9	7	4	4	4

F: Frontal, T :Temporal, P: Parietal, O: Occipital, CE: Cerebellar, CV: Cervical, T:Tohoracic, L: Lumbar

Table 6. Histopathological findings of subpial tissue according to the regions of group-III.

Histopathological findings (n=10)	F	T	P	O	CE	CV	T	L
Edema	5	5	5	8	6	4	8	3
Congestion	5	5	5	8	6	4	7	3
Increasing in collagen	7	7	5	9	5	5	9	6
Thickening of basal lamina	7	6	4	9	6	5	7	4
Opening desmosomes	6	5	5	9	6	6	7	5
Opening hemidesmosomes	6	6	6	9	5	4	7	6
Opening gap-junctions	7	6	4	9	6	5	8	4
Opening tight-junctions	6	5	5	9	7	4	9	5
Vasculitis	5	5	5	7	5	3	9	3
Myelin degeneration	7	6	4	9	6	5	9	6

F: Frontal, T :Temporal, P: Parietal, O: Occipital, CE: Cerebellar, CV: Cervical, T:Tohoracic, L: Lumbar

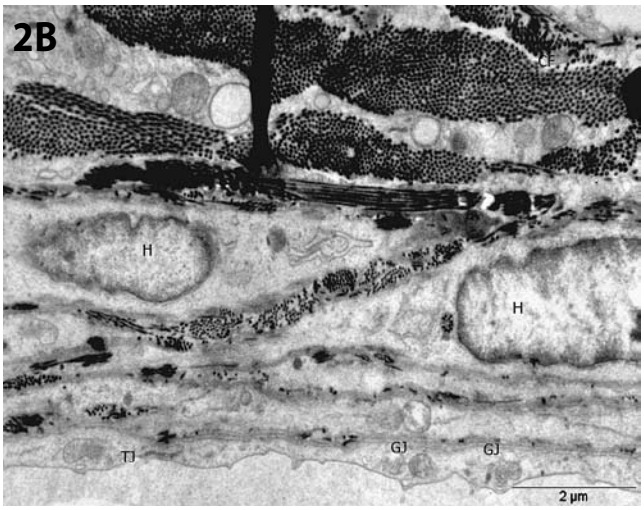

Figure 2A. Electronmicrograph of a rat of group-III in occipital region. Pial cells (PLC), vasculitis and degeneration of subpial tissue (D) are observed. Bar 10 µm. Uranyl acetate and lead citrate ×3 000.

Figure 2B. Electronmicrograph of a rat of group-III at thoracic level. Separation of tight junctions (TJ) and gap junctions (GJ), and diffuse collagen fibers accumulation are shown. Bar 2 µm. Uranyl acetate and lead citrate ×12 000.

Histologically, pia mater is largely made up of flattened connective tissue cells (pial cells) [10]. Pia mater is seen as a delicate and, apparently continuous cellular layer which is joined by desmosomes and other specialized junctional apparatus under TEM [19]. Despite the multiple anatomical arrangements and physiological functions, leptomeningeal cells retain many histological features that are similar from site to site [25]. Generally, the spinal and cranial meninges are supposed to have a similar fine structured organization in human [11,24].

In leptomeningitis, PMNLs and macrophages are distributed throughout the subarachnoid, subpial and perivascular spaces. The wide distribution of the inflammatory cells indicates that they are able to migrate from the blood vessel lumina, through the vascular endothelium, into the perivascular space and to pen-

etrate the pia on the surface of the brain or to transverse the arachnoid coating of the subarachnoid vessels [5,8].

The alterations of blood brain barrier (BBB) permeability during development of experimental meningitis may vary for different models of inducing meningitis and that the mechanisms responsible for these different permeability changes may be multifactorial [7]. The pia mater seems to be well suited for immune response mechanism and inflammatory reactions [3]. But it is suggested that the fine anatomy of the human spinal meninges significantly different from the other mammals [11,25]. Reina MA et al studied the ultrastructural anatomy of the pia mater, such as pial cells, membrane thickness and subpial tissue at distinct levels of the thoracic and lumbar spinal cord and nerve roots [19].

Animal models have been used extensively during the past two decades to increase our comprehension of the pathogenesis and pathophysiology of bacterial meningitis [23]. The ideal animal model should be simple and reproducible with an initiating insult via a route and of a level suitable to that seen in a clinical setting [13]. Previously employed models have generally been designed in order to rely on the direct intracisternal inoculation of bacteria for induction of infection [18,21,23]. As a result of this, natural bacteriemia-meningitis sequence is bypassed and an artificial pathogenesis is developed. On the contrary, most cases of bacterial meningitis arise as a consequence of hematogenous spread [23]. Non-systemic challenge techniques such as intranasal instillation of bacteria may result in inconsistent mortality rates [2]. The presented model in this study has an advantage over previous ones according to its direct bacteriemia characteristic. As organ dysfunctions may occur independently of invasion of the organ by circulating bacteria in the course of sepsis [15], it can be speculated that, alterations of permeability of blood brain barrier (BBB) may happen before bacterial invasion; and pathogenetic mechanism might change. Increased permeability of BBB may make bacterial invasion easier. The other factors that make this invasion straightforward are opening junctional structures and perimicrovascular edema formation [13,22]. As a result of this, pathophysiologic consequences of hematogenous bacterial meningitis after organisms have reached the subarachnoid space might be more natural. The other advantage of the presented model is that it supplies the uniform concentration of bacteria in the circulation. The sites of CNS invasion may change by challenging bacteria intracisternally. Consequently, detecting the most vulnerable zones of the CNS that is one of the important results of this study can not be obtained by using previous models. Nearby structures which the cistern is inoculated with bacteria might tend to be more affected; and they may exhibit different levels of invasion.

Meningitis-associated nervous tissue injury is not mediated only by the existence of viable bacteria, but occurs as a consequence of the host reaction to bacterial components [20]. Obtaining uniform host response to experimental meningitis at the level of leptomeningeal and subpial tissues should be one of the mainstays of the experiment designed to evaluate the histopathological changes. Achieving the same results in detecting the most vulnerable sites of the CNS and histopathological finding are seen mostly, via two different ways (ip and iv) of challenging bacteria which make our model more reliable.

CONCLUSION

It can be concluded that occipital and thoracic regions are the most vulnerable sites to inflammations developing in the course of systemic *S. aureus* infections. It may also be said that an increase in collagenous tissue is the most detected inflammatory reaction of the leptomeninges and subpial area during *S. aureus* bacteriemia. This experimental *S. aureus* meningitis model can be used to induce subpial and leptomeningeal inflammations and it might be utilized for investigations of pathogenesis of leptomeningitis during systemic infections.

REFERENCES

1 Dacey RG, Sande MA. Effect of probenecid on cerebrospinal fluid concentrations of penicillin and cephalosporin derivatives. Antimicrob Agents Chemother. 1974; **6**: 437–444.
2 Davies DC. Blood-brain barrier breakdown in septic encephalopathy and brain tumours. J Anat. 2002; **200**: 639–646.
3 Fricke B, Andres KH, Von During M. Nerve fibers innervating the cranial and spinal meninges: morphology of nerve fiber terminals and their structural integration. Microsc Res Tech. 2001; **53**(2): 96–105.
4 Hirst RA, Gosai B, Rutman A, Andew PW, O'Callagan C. Streptococcus pneumoniae damages the ciliated ependyma of the brain during meningitis. Infection and Community. 2003; **71**(10): 6095–6100.
5 Hutchings M, Weller RO. Anatomical relationships of the pia mater to cerebral blood vessels in man. J Neurosurg. 1986; **65**(3): 316–25.
6 Kida S, Yamashima T, Kubota T, Ito H, Yamamoto S. A light and electron microscopic and immunohistochemical study of human arachnoid villi. J Neurosurg. 1988; **69**(3): 429–35.
7 Kim KS, Wass CA, Cross AS. Blood-brain barrier permeability during the development of experimental bacterial meningitis in the rat. Exp Neurol. 1997; **145**(1): 253–7.
8 Koedel U, Pfister HW. Models of bacterial meningitis: role and limitations. Infect Dis Clin North Am. 1999; **13**(3): 549–77.
9 Leib SL, Tauber MG. Pathogenesis of bacterial meningitis. Infect Dis Clin North Am. 1999; **13**(3): 527–48.
10 Morse DE, Low FN. The fine structure of the pia mater of the rat. Am J Anat. 1972; **133**(3): 349–67.
11 Nicholas DS, Weller RO. The fine anatomy of the human spinal meninges. A light and scanning electron microscopy study. J Neurosurg. 1988; **69**(2): 276–82.
12 Oda Y, Nakanishi I. Ultrastructure of the mouse leptomeninx. J Comp Neurol. 1984; **225**(3): 448–57.
13 Orihuela CJ, Fillon S, Smith-Sielicki SH, El Kasmi KC, Gao G, Soulis K, Patil A, Murray PJ, Tuomanen EI. Cell wall-mediated neurnal damage in early sepsis. Infect Immun. 2006; **74**(7): 3783–3789.
14 Østergaard C, Yieng-Kow RV, Knudsen JD, Frimodt-Møeller N, Espersen F. Evaluation of fusidic acid in therapy of experimental *Staphylococcus aureus* meningitis. JAC. 2003; **51**: 1301–1305.
15 Parker SJ, Watkins PE. Experimental models of gram-negative sepsis. British J Surg. 2001; **88**: 22–30.

16 Petty MA, Lo EH. Junctional complexes of the blood-brain barrier: permeability changes in neuroinflammation. Progress in Neurobiology. 2002; **68**: 311–323.
17 Pintado V, Meseguer MA, Fortun J, Cobo J, Navas E, Quereda C, Corral I, Moreno S. Clinical study of 44 cases of *Staphylococcus aureus* meningitis. Eur J Clin Microbiol Infect Dis. 2002; **21**: 864–868.
18 Quagiarello VJ, Long WJ, Scheld WM. Morphologic alteration of the Blood-brain barrier with experimental meningitis in rat. J Clin Invest. 1986; **77**: 1084–1095.
19 Reina MA, De Leon COL, Villanueva MC, Lopez A, Maches F, De Andres JA. Ultrastructural findings in human spinal pia mater in relation to subarachnoid anesthesia. Anesth Analg. 2004; **98**(5): 1479–85.
20 Scheld WM, Koedel U, Nathan B, Pfister HW. Pathophysiology of bacterial meningitis: Mechanism(s) of neuronal injury. JID. 2002; **186**(Suppl 2): S225–33.
21 Sipahi OR, Arda B, Yurtseven T, Sipahi H, Ozgiray E, Suntur BM, Ulusoy S. Vancomycin versus teicoplanin in the therapy of experimental methicillin-resistant *Staphylococcus aureus* (MRSA) meningitis. Int J Antimicrobiol Agents. 2005; **26**: 412–415.
22 Tsai YH, Bies M, Leitner F, Kessler RE. Therapeutic studies of cefepime (BMY 28142) in murine meningitis and pharmacokinetics in neonatal rats. Antimicrob Agents Chemother. 1990; **34**(5): 733–738.
23 Tunkel AR, Scheld WM. Pathogenesis and pathophysiology of bacterial meningitis. Clin Microbiol Rev. 1993; **6**: 118–136.
24 Vandanabeele F, Creemers J, Lambrichts I. Ultrastructure of the human spinal arachnoid mater and dura mater. J Anat. 1996; **189**(Pt 2): 417–30.
25 Weller RO. Microscopic morphology and histology of the human meninges. Morphologie. 2005; **89**(284): 22–34.
26 Zhang ET, Inman CB, Weller RO. Interrelationships of the pia mater and the perivascular (Virchow-Robin) spaces in human cerebrum. J Anat. 1990; **170**: 111–23.